34th Annual International Conference of the IEEE EMBS
San Diego, California USA, 28 August - 1 September, 2012

A Low noise, Non-contact Capacitive Cardiac Sensor*

GuoChen Peng[1] and Mark F. Bocko[1]

Abstract— **The development of sensitive, non-contact electric field sensors to measure weak bioelectric signals will be useful for the development of a number of unobtrusive health sensors. In this paper we summarize our recent work on a number of specific challenges in the development of non-contact ECG sensors. First, we considered the design of a low noise sensor preamplifier. We have adapted circuit designs that incorporate a double feedback loop to cancel the input transistor leakage current while providing stable operation, fast settling time and good low frequency response without the need for ultrahigh value resistors. The measured input referred noise of the preamplifier in the frequency band 0.05-100 Hz is 0.76 μV_{rms}, which is several times lower than existing ECG preamplifiers.**

I. INTRODUCTION

Sensors and systems for electrocardiogram (ECG) measurements have been developed and refined for many years. The front-end of all ECG systems consists of the sensor electrodes and preamplifiers. Traditional adhesive sensor electrodes provide a stable, low impedance signal source that allows for the low-noise measurement of ECG signals but the wires and adhesives employed are unsuitable for long term use, even common 24-48 hour Holter monitoring sessions are a considerable inconvenience and discomfort to the user so longer term personal health monitoring with traditional adhesive electrodes would be unworkable. Therefore, the development of non-contact ECG sensors that may be built into emergency medical equipment, examining tables, beds or other furniture is an attractive option [1].

Junction field effect transistors (JFETs) are usually the devices of choice for low noise applications when the signal source impedance is large. The typically high transconductance of JFETs gives a low noise floor, however, a major problem in using JFETs in operational amplier designs is the bias current instability with temperature drift. This in turn may cause a voltage offset problem. There are several techniques to reduce offset voltage including chopper architectures [2] and the auto-zero topology [3]. In addition, the fluctuations of the input leakage current of the JFET pn junction may make a large noise contribution for high impedance signal sources, i.e., small source capacitance. To address these problems, a charge amplifier with a double feedback was explored in this work.

In the following section we present the preamplifier design and an analysis. In Section III and IV we present the experimental results, which are followed by a brief conclusion.

*This work was supported by Blue Highway and the New York State Foundation for Science, Technology and Innovation.

[1]G.Peng and M. F. Bocko are with the Electrical and Computer Engineering Department, University of Rochester, Rochester, NY 14627-0231 USA gupeng;bocko at ece.rochester.edu

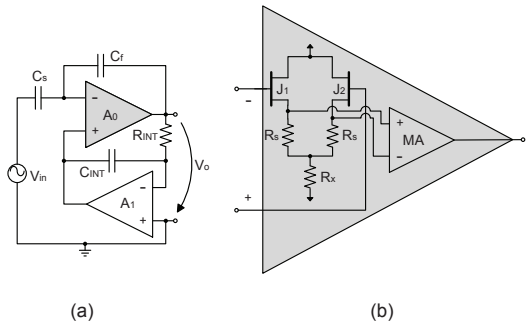

Fig. 1. (a) Input leakage current compensated charge amplifier employing a double feedback loop. In (b) the composite amplifier A_0 is shown in detail, it is composed of an input differential JFET pair in a common drain configuration followed by a low noise monolithic amplifier, MA.

II. PREAMPLIFIER DEVELOPMENT

A. Input Leakage Current Compensated Charge Amplifier(ILC3A)

The proposed cardiac preamplifier is shown in Fig. 1. This shows a charge amplifier with a capacitive transducer (with input voltage source V_{in} and source capacitance C_s) at its input. The charge amplifier consists of a composite amplifier A_0 and a feedback capacitor C_f. There also is a feedback integrator with R_{INT}, C_{INT}, and an operational amplifier A_1. The composite amplifier A_0 employs an input JFET common drain differential pair followed by a low noise monolithic amplifier, labeled MA. Note that this is different from the JFET source follower preamplifier that is commonly used as a buffer amplifier for biomedical signals. The ILC3A amplifier configuration simultaneously achieves good low frequency response, high gain, and leakage current compensation without the need for high value resistors or high input impedance which is required by normal preamplfiers.

B. Frequency Response and Noise Analysis

The gain of the ILC3A circuit shown in Fig. 1 is given in (1) and is dominated by the ratio of the signal source capacitance, C_s and the first-stage feedback capacitor, C_f

$$Gain = \left(\frac{-C_s}{C_f}\right) \cdot \frac{s}{s+\omega_0} \tag{1}$$

in which the high-pass corner frequency, ω_0, is given by $\omega_0 = (1/R_{INT}C_{INT})\cdot(1+C_s/C_f)$, where $s = j\omega$ and ω is the frequency in radians/sec. This high-pass characteristic is useful in an ECG amplifier to filter out low-frequency signals due to subject motion during respiration. Moreover, the settling time may be improved by increasing the value

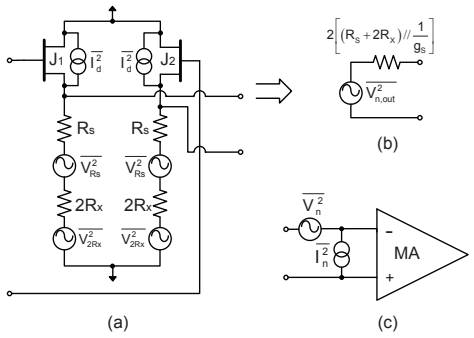

Fig. 2. In (a) is shown the noise model of the JFET pair in the composite amplifier A_0 of Fig. 1. The circuit in (a) can be reduced to the equivalent circuit in (b) with a single voltage noise source $\overline{V_{n,out}^2}$ in series with an equivalent resistance. The noise equivalent circuit of the monolithic amplifier (MA) that follows the JFET pair in the composite amplifier is shown in (c).

of C_s while trading off the high-pass corner frequency. Specifically, for C_s = 1000 pF with the product of R_{INT} and C_{INT} is 6.05 sec, the settling time can be 2.35 seconds and high-pass corner frequency is about 0.06 Hz; for C_s = 1 pF, settling time is about 18 seconds while the HP corner frequency is 0.009 Hz.

The primary advantage of the ILC3A is that the feedback signal to transistor J_2 stabilizes the output voltage of A_0 by driving the input transistor J_1 gate leakage current to zero. Temperature drift of J_1 leads to a change in the J_1 gate input leakage current, which in turn, causes the output of A_0 to drift. In the feedback configuration shown in Fig. 1 the leakage current from J_1 is integrated on capacitor C_f and this signal then drives the A_1 amplifier and the C_{INT} feedback loop. The signal from A_1 drives the gate of J_2, which changes the voltage across R_x causing the drain-source current of J_1 to change in a direction that forces the J_1 gate-source voltage toward zero, thereby eliminating the leakage current. The effectiveness of the method relies on J_1 and J_2 being matched, which is a good assumption for monolithically fabricated matched JFET pairs. The inverting feedback loop also cancels low-frequency signals from the capacitive sensor and low-frequency noise from A_0 to achieve stable operation.

The noise analysis of the ILC3A can be divided into a few steps. We begin with an analysis of the composite operational amplifier A_0. In the model shown in Fig. 2(a), with the assumption that all noise sources are mutually uncorrelated, the mean squared output noise of the JFET common drain differential pair is

$$\begin{aligned}\overline{V_{n,out}^2} &= 2\left(4kT(2R_x)\right) + 2\left(4kTR_s\right) \\ &\quad + 2\left(4kT(\frac{2}{3})g_s\right)\left[(R_s+2R_x)//\left(\frac{1}{g_s}\right)\right]^2 \quad (2)\end{aligned}$$

where g_s is the forward transconductance of the J_1 and J_2 transistors (assumed to be matched), k is Boltzmann's constant, and T is the temperature in degrees Kelvin. The first two terms in (2) are the Johnson noise contributed from R_x and R_s, and the third term represents the thermal noise of the JFET channel.

Equivalent circuit models of noisy two-port devices, such as the amplifier in Fig. 2(a), normally contain two noise sources: a purely additive voltage noise source and an input current noise source. In the present case the input current noise is ignored. The input current noise would be due to two sources, the shot noise associated with the JFET input leakage current and the JFET channel current noise coupled back to the input through the gate-channel capacitance [4]. Since the input leakage current is forced to zero by the feedback, the input leakage associated shot noise, which is proportional to the magnitude of the leakage current, also is zero. Furthermore, the gate-drain capacitance is very small so the second source of input noise is negligible. Therefore in our model the input current noise is omitted entirely.

The noise of the input JFET pair can be combined with that of the following monolithic amplifier MA shown in Fig. 2(c). The total noise of the composite amplifier referred to the input of MA is then,

$$\begin{aligned}\overline{V_{n,out\_total}^2} &= \overline{V_{n,out}^2} + \overline{V_n^2} \\ &\quad + 2\overline{I_n^2}\left((R_s+2R_x)//\left(\frac{1}{g_s}\right)\right)^2 \quad (3)\end{aligned}$$

The second and third terms are respectively the additive voltage noise and the input current noise contributed by the following amplifier, MA.

The total noise referred back to the JFET input, $\overline{V_{n,in}^2}$, is

$$\overline{V_{n,in}^2} = \overline{V_{n,out\_total}^2}/G^2 \quad (4)$$

where G is given by $G = (R_s+2R_x)/(R_s+2R_x+1/g_s)$. $\overline{V_{n,in}^2}$ is thermal in origin and thus has a "white" spectrum. The $1/f$ noise of the JFET may be included empirically by adding a term, K_v^2/f, to the input referred noise spectral density; thus the total noise of A_0 is (expressed as a noise spectral density)

$$S_{v\_tot} = \overline{V_{n,in}^2} + K_v^2/f \quad (V^2/Hz) \quad (5)$$

Typically, the low frequency noise in a JFET is dominated by $1/f$ noise [4] and the constant K_v must be empirically determined.

The noise at the non-inverting terminal of the composite amplifier arises from the feedback integrator A_1. The noise at the integrator output is given by,

$$\begin{aligned}\overline{V_{n,INT}^2} &= \left(\overline{I_{R_{INT}}^2} + \overline{I_{n1}^2}\right)\left(\frac{1}{sC_{INT}}\right)^2 \\ &\quad + \overline{V_{n1}^2}\left(1+\frac{1}{sR_{INT}C_{INT}}\right)^2 \quad (6)\end{aligned}$$

where $\overline{I_{R_{INT}}^2}$ is the integrating resistor current noise and $\overline{I_{n1}^2}$ and $\overline{V_{n1}^2}$ are respectively the current and voltage noise of the monolithic amplifier A_1. Finally, under the assumption that the various noise sources are mutually uncorrelated, the total

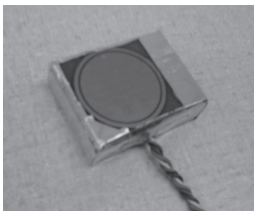

Fig. 3. Non-contact capacitive sensor and electronics package in which the electrode with a diameter of 3 cm was fabricated from standard FR-4 printed circuit board material surrounded by a guard-ring to reduce the stray capacitance to ground and to shield from stray electric fields.

input referred noise of the entire preamplifier is given by the following expression,

$$\overline{V^2_{n,in\_tot}} = \left(\overline{V^2_{n,INT}} + \overline{V^2_{n,in}}\right)\left[\frac{(C_s + C_f + C_{in})}{C_s}\right]^2 (rms) \tag{7}$$

C. Noise Simulation

The OP27 amplifier [5] was chosen for MA and A_1. The feedback capacitance C_f was 30 pF to give a reasonable gain value for typical ECG electrode capacitances and R_s and R_x are 1k and 10k ohms respectively. The sensor capacitor plate was fabricated from standard copper printed circuit board; the copper electrode has a polymer over-layer of thickness 0.18 mm with a relative permittivity of 4.5 (see Fig. 3). A 2N4338 JFET [6] was selected for its low noise due to its high transconductance of 1.8 mS. R_{INT} and C_{INT} are 805 kOhms and 100 μF respectively, which gives a low frequency cutoff around 0.005 Hz. Based upon these parameters the noise power spectral density of the various individual sources was simulated, the noise contributed by the OP27 and the feedback integrator over the frequency band of interest are both small in comparison to the input noise of the JFET differential pair, thus only the noise from the JFET differential pair needs to be considered. Moreover, higher source capacitance leads to decreased source input-referred noise.

III. NOISE MEASUREMENT

The ILC3A preamplifier noise was measured with the prototype sensor shown in Fig. 3. The discrete component values for the charge preamplifier were the same as those in the simulation. In order to measure the noise of the ILC3A, a 500x high gain, low noise amplifier (LNA) was inserted between the ILC3A and a National Instruments NI-USB6009 data collection board. The source capacitance was measured in situ by an auxiliary capacitance bridge for each noise measurement. The input referred noise of the ILC3A is plotted in Fig. 4. Also shown on the plot is the predicted noise, based upon the known and measured device and circuit parameters. The overall equivalent noise referred to the signal source terminal is 0.76 μV_{rms} integrated over a frequency band from 0.05 to 100 Hz for a measured source capacitance of 21 pF.

To verify the effectiveness of the transistor leakage current cancellation of the system, we shorted the preamp source

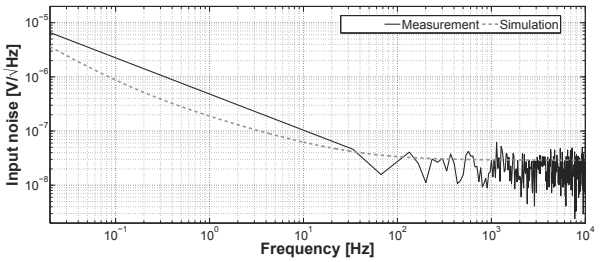

Fig. 4. Measured (solid line) and simulated (dotted line) input referred noise spectral density for the charge preamplifier design shown in Fig. 1. The measured noise contributions from the LNA and NI data acquisition card were subtracted. It is noted that the $1/f$ noise simulation parameter can be determined from the JFET datasheet.

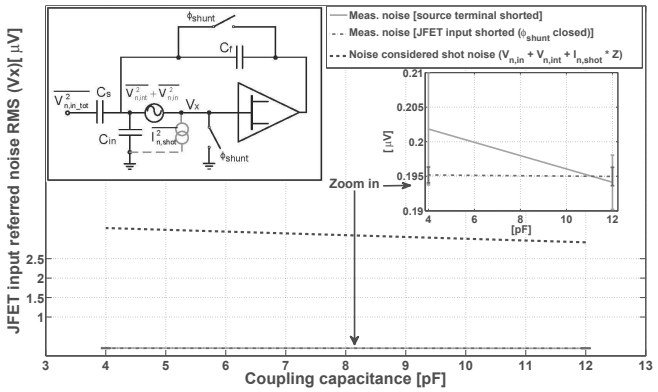

Fig. 5. Noise at the JFET input, V_x, (measured over 1-100Hz frequency band) recorded at 2 different electrode-to-subject coupling capacitances (4 pF and 12 pF). In the zoomed plot, the error bar was inferred from 25 measurements for each case. The measured noise is at least 16x less than the value that would be inferred from the leakage current induced noise (shown by the bold dotted line.) This is due to the leakage current suppression of the ILC3A amplifier, which in turn reduces the input current noise.

terminal and measured the output noise, which can then be inferred to the input to the JFET using the transfer function from the output back to JFET input, $C_f/(C_s + C_{in} + C_f)$. A total of 25 noise measurements were made at each of two different input capacitance values, 4 pF and 12 pF. In Fig. 5, the result shows that the noise level is approximately 0.2 μV_{rms} in a 1-100 Hz bandwidth. We note that this result is about 16x smaller than the noise one would predict considering the shot noise contributed by the leakage current given in the JFET datasheet [6], $I_{n,shot}$, and the impedance $Z = 1/s(C_s + C_{in} + C_f)$, at the input to the JFET. This is because the amplifier configuration drives the leakage current to near zero, which in turn reduces the input current noise. This means then that the total noise is primarily from the voltage noise contributions $V_{n,int}$ and $V_{n,in}$ in (4) and (6). Also, we introduced a switch ϕ_{shunt} (shown in the figure) to short the JFET input to obtain $V_{n,int}$ and $V_{n,in}$ directly. It was found that the difference in the measured noise with the JFET input shorted and then connected to the capacitive source terminal, are small (for example, less than 0.001 μV_{rms} for an input capacitance of 12 pF.) This then demonstrates that the leakage current noise is greatly reduced by the double feedback preamplier conguration.

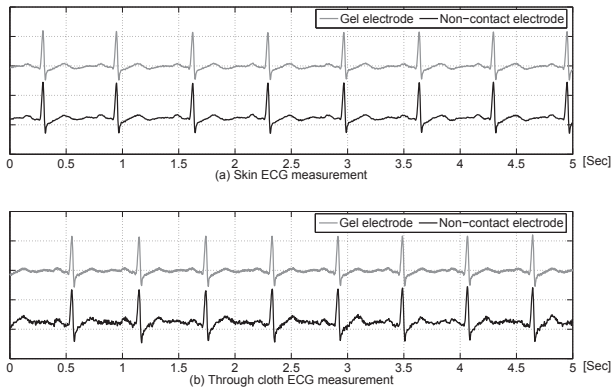

Fig. 6. ECG measurements on (a) skin and (b) clothing obtained with the sensor shown in Fig. 3. The upper trace was measured with commercial Ag/AgCl electrodes; the lower trace was measured with the non-contact sensor.

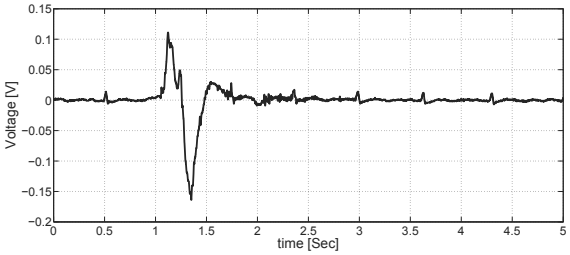

Fig. 7. Movement of the non-contact electrode leads to baseline wandering. Note that the baseline shifts may be much larger than the ECG signal; also note the small R peaks throughout the trace. It takes about 2.5 sec to recover. From this observed settling time the inferred source capacitance is approximately 930 pF. (For C_f = 30 pF)

TABLE I
INPUT REFERRED NOISE VOLTAGE OF VARIOUS PREAMPLIFIER DESIGNS

RMS input noise	Denison [7]	Yazicioglu [8]	Prance [9]	Smith [10]	This work
$\mu V_{(5-35\ Hz)}$	-	-	6.3	45	0.46
$\mu V_{(0.05-100\ Hz)}$	0.98	0.85	-	-	0.76

Without using the leakage current nulling technique, the current noise contribution for large source impedances (small capacitances) would dominate the overall noise.

IV. ECG SIGNAL MEASUREMENT

Non-contact ECG signals were recorded using the standard lead II electrode placement. One sensor was placed below the clavicle on the right shoulder of the subject and the other on the subjects abdomen; both sensors interfaced with the subject through the subjects clothing. The reference was defined by the potential of the subject's left wrist, far from the precordial area. The differential amplifier was a Texas Instruments INA116 low noise instrumentation amplifier with a gain of 11. A digital bandpass filter was applied to the signal to provide a 1-100 Hz bandwidth, and a notch filter was used to attenuate 60 Hz line pickup. The entire system was run from battery supplies. We also simultaneously recorded the ECG signal using conventional Ag/AgCl gel electrodes placed close to each corresponding non-contact sensor. Fig. 6 shows the output signals of both the non-contact and the conventional contacting ECG sensors. The R-R interval (heart rate) and details of the QRS complex are clearly recognizable in both. In Fig. 7 an ECG trace is shown in which the electrode moved at t = 1 sec; the trace displays a transient recovery time of about 2.5 seconds which is in agreement with the predicted transient recovery time (section II-B).

V. CONCLUSIONS

A low noise non-contact ECG sensor preamplifier has been developed and characterized. It employs a JFET input differential pair and dual feedback loops. This preamplifier design has several advantages over previous designs. First, it eliminates the large-value feedback resistor, while still providing good low-frequency response and cancellation of the JFET gate input leakage current, which was a source of drift in previous designs. Modeling and measurements show that it is possible to obtain these practical advantages and a noise level that is much less than previously reported results for low-noise pre-amplifiers coupled to electric potential probes in physical contact with the subject, see Table I for a comparison. It is worth noting that in the small source capacitance regime, the low noise charge amplifier may give a higher signal to noise ratio than a voltage amplifier readout. Of course, in the final system design issues such as the source impedance dependence of the current mode preamplifier gain and the common mode rejection ratio (CMRR) must be addressed and is the subject of ongoing work.

REFERENCES

[1] A. Aleksandrowicz and S. Leonhardt, "Wireless and non-contact ecg measurement system -the "aachen smartchair"," *Acta Polytechnica*, vol. 47, no. 4-5, pp. 58–71, 2007.

[2] A. Bakker, K. Thiele, and J. Huijsing, "A cmos nested-chopper instrumentation amplifier with 100-nv offset," *Solid-State Circuits, IEEE Journal of*, vol. 35, no. 12, pp. 1877 –1883, dec 2000.

[3] I. Finvers, J. Haslett, and F. Trofimenkoff, "A high temperature precision amplifier," *Solid-State Circuits, IEEE Journal of*, vol. 30, no. 2, pp. 120 –128, feb 1995.

[4] F. Levinzon, "Noise of the jfet amplifier," *Circuits and Systems I: Fundamental Theory and Applications, IEEE Transactions on*, vol. 47, no. 7, pp. 981 –985, jul 2000.

[5] *Low-Noise, precision operational amplifier*, ANALOG DEVICES, 2003.

[6] *N-Channel JFET*, Vishay Siliconix, 2001.

[7] T. Denison, K. Consoer, W. Santa, A.-T. Avestruz, J. Cooley, and A. Kelly, "A 2 uw 100 nv/rthz chopper-stabilized instrumentation amplifier for chronic measurement of neural field potentials," *Solid-State Circuits, IEEE Journal of*, vol. 42, no. 12, pp. 2934 –2945, dec. 2007.

[8] R. Yazicioglu, S. Kim, T. Torfs, H. Kim, and C. Van Hoof, "A 30 w analog signal processor asic for portable biopotential signal monitoring," *Solid-State Circuits, IEEE Journal of*, vol. 46, no. 1, pp. 209 –223, jan. 2011.

[9] C. J. Harland, T. D. Clark, and R. J. Prance, "Electric potential probes - new directions in the remote sensing of the human body," *Measurement Science and Technology*, vol. 13, no. 2, p. 163, 2002.

[10] W. Smith and J. LaCourse, "Non-contact biopotential measurement from the human body using a low-impedance charge amplifier," in *Bioengineering Conference, 2004. Proceedings of the IEEE 30th Annual Northeast*, april 2004, pp. 31 – 32.